LETTER

Strain-modulated photoelectric properties of self-rolled GaAs/$Al_{0.26}Ga_{0.74}As$ quantum well nanomembrane

Applied Physics Express 12, 065003 (2019)
https://doi.org/10.7567/1882-0786/ab2161

LETTER

Strain-modulated photoelectric properties of self-rolled GaAs/$Al_{0.26}Ga_{0.74}As$ quantum well nanomembrane

Fei Zhang[1], XiaoFei Nie[2], GaoShan Huang[1*], HongLou Zhen[2], Fei Ding[3], ZengFeng Di[4], and YongFeng Mei[1*]

[1]Department of Materials Science, State Key Laboratory of ASIC and Systems, Fudan University, Shanghai 200433, People's Republic of China
[2]State Key Laboratory of Infrared Physics, Shanghai Institute of Technical Physics, Chinese Academy of Sciences, Shanghai 200083, People's Republic of China
[3]Institut für Festkörperphysik, Leibniz Universität Hannover, Appelstrasse 2, 30167, Hannover, Germany
[4]State Key Laboratory of Functional Materials for Informatics, Shanghai Institute of Microsystem and Information Technology, Chinese Academy of Sciences, Shanghai 200050, People's Republic of China

*E-mail: gshuang@fudan.edu.cn; yfm@fudan.edu.cn

Received March 29, 2019; revised May 5, 2019; accepted May 13, 2019; published online May 23, 2019

In this study, we investigate the effects of stress/strain on the band structures of self-rolled GaAs/$Al_{0.26}Ga_{0.74}As$ quantum wells (QWs). The results show that the two QWs are in different stress/strain statuses and the boundary line locates between the two QWs. Based on spectral characterizations under different bias voltages, we disclose that interface polarization exists in self-rolled nanomembrane. In addition, we find that the responsivity of the QW in tensile strain is higher than that in compressive strain, and therefore we fabricated a self-rolled-down tubular structure with both two QWs in tensile strain to increase the responsivity by ~52%. © 2019 The Japan Society of Applied Physics

Supplementary material for this article is available online

The infrared detectors based on GaAs/AlGaAs quantum well (QW) structures have outstanding performance, such as adjustable continuous wavelength, low cost, and excellent radiation resistance.[1–3] The properties of semiconductor QW are essentially related to the band structure of the functional layer and the transport properties of carriers within the energy bands. Generally, the action for the external electromagnetic field, the structure size, and the incident photons on the electron transport and optical phenomena are studied based on the energy-band engineering and strain engineering for the QW structures.[4–7] Therefore, the study concerning band regulation is of great significance for promoting the performance of semiconductor QW devices.

Combining the rolled-up nanotechnology with the QW infrared detector, where the flexible nanomembrane containing the QW structure is self-rolled into tubular structure, can greatly enhance the light absorptivity compared with the plane film.[8–10] Moreover, our previous investigation showed that the tubular detector has a wider response angle and better stability.[10] Since the strain in nanomembrane can affect the energy band structure of the QW, the physical properties and performance of the self-rolled nanomembrane and the device, where the strain is re-balanced in the self-assembly process, are significantly influenced and modulated.[11–17] In this work, we combine experimental study with theoretical analyses to investigate the photoelectric characteristics of self-rolled QW infrared photodetectors by regulating the stress/strain status of the QW layer. The change of energy band caused by the stress/strain and its effect on the carrier transition therein is specifically analyzed. The results obtained in this work pave the way for fabricating stable and reliable photodetectors with controllable wavelength, wide response angle, and high sensitivity.

The sample structure is AlAs/$In_{0.2}Al_{0.2}Ga_{0.6}As$/GaAs/QWs/GaAs multi-layer from bottom to top where QWs represents GaAs/$Al_{0.26}Ga_{0.74}As$ with double cycles (Fig. 1). During the molecular beam epitaxial growth, ~200 nm GaAs buffer layer was firstly deposited on GaAs(100) substrate and then followed by 30 nm AlAs sacrificial layer and 20 nm $In_{0.2}Al_{0.2}Ga_{0.6}As$ strain layer. Then a 50 nm GaAs followed as the conductance layer connected to the bottom electrode. We then deposited 30 nm $Al_{0.26}Ga_{0.74}As$ as the potential barrier layer and 6.5 nm GaAs as the potential well layer for the two QWs, above which 20 nm GaAs was deposited as the conductance layer for upper electrode (left panel of Fig. 1). By using the conventional IC planar technology, the electrodes (AuGe/Ni/Au) were deposited on the top (positive bias) and bottom (negative bias) contact layers to enable an electrical access. When the AlAs sacrificial layer was chemically etched away with HF solution, the above multi-layered nanomembrane self-rolled by the action of strain layer due to the energy miniaturization of the system.[18,19] In this work, the sacrificial layer was removed in dilute HF solutions with concentrations of 18%, 15%, 13%, and 10% and the corresponding diameters of the self-rolled-up tubular structures are 158, 150, 127, and 62 μm respectively. The change in the diameter is considered to be connected with the different strain relaxation processes under varied corrosion rates because the strain gradient changes with the distance from the etching front.[20]

The photocurrent spectra of the devices at low temperature were obtained by illuminating the device with a Fourier transform infrared spectrometer (Nicolet 6700). The blackbody responses were collected by illuminating the sample with a thermal source at 800 K. The photoluminescence (PL) spectroscopy was also carried out with LabRAM HR spectrometer equipped with 540 nm laser.

Figure 2(a) shows the normalized photocurrent spectra of flat nanomembrane and self-rolled-up nanomembranes with different diameters. It is worth noting that the spectrum of flat nanomembrane demonstrates one broad band while in the case of self-rolled-up nanomembrane, a shoulder peak can easily be distinguished. The results suggest that the strain/stress in the nanomembrane lead to different optical transitions in two QWs. This can be explained by strain variation as follows. In the self-rolled-up nanomembrane, the tangential strain changes along the vertical position,[13] and the corresponding band structures can be calculated by the

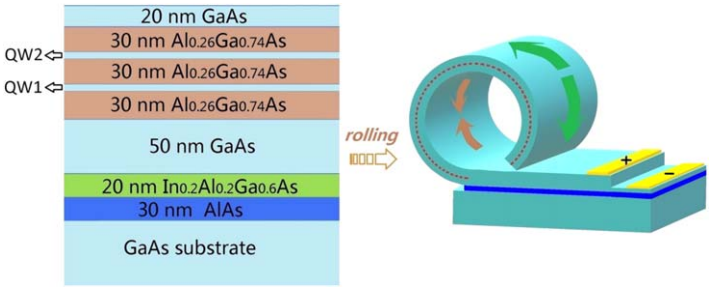

Fig. 1. (Color online) Schematic diagram of a self-rolled-up nanomembrane. The outer surface of the tube is tensile-strained, while the inner is compressive-strained. By removing the AlAs sacrificial layer (blue color), the above nanomembrane rolls up to minimize the total elastic energy.

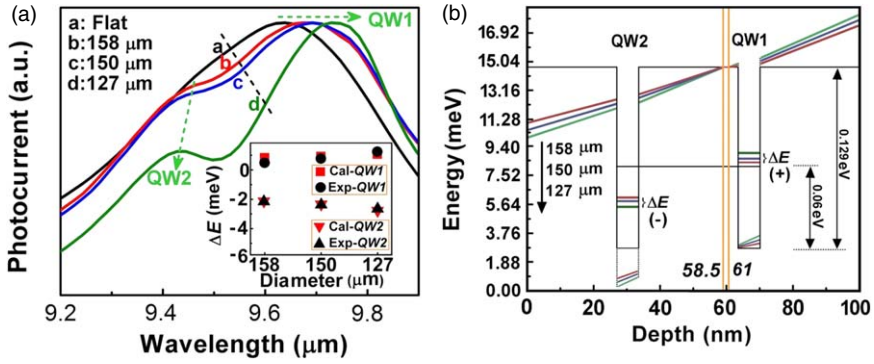

Fig. 2. (Color online) (a) Normalized photocurrent spectra of flat and self-rolled nanomembranes with different diameters. The spectra were collected at 40 K. The inset indicates the shift of the energy level (e_0) of QWs in nanomembranes. Both calculated and experimental values are presented. The rolling leads to redshift of the energy level in QW1, and blueshift of the energy level in QW2. (b) Band structures of self-rolled-up nanomembranes with different diameters. The yellow lines present the position range of boundary lines of compressed and tensed statuses. The curvature change leads to small variation of the energy level, and the left coordinate was used to magnify this variation.

deformation potential theory.[21] The results demonstrate that the energy level shifts in the rolled-up nanomembrane and a tilted energy level should exist with the increasing depth, which can be identified on the right coordinate of Fig. 2(b). The flat nanomembrane can be regarded as tube with infinite diameter, and the two QWs are under the same strain statuses. As a result, the energy levels in the two QWs are the same and only one broad band is observed in Fig. 2(a).

However, the broad band with two sub-peaks is in the self-rolled-up nanomembranes and the smaller the diameter is, the bigger the space between the two sub-peaks is. In addition, the left peak gradually blueshifts, while the right peak redshifts as the radius decreases. It suggests that the two QWs have different energy levels. According to the deformation potential theory,[21] we can calculate the positions of boundary lines of three different self-rolled-up nanomembranes and find the positions of boundary lines are in the range of 58.5 to 61 nm (see yellow lines in Fig. 2(b) and supplementary material A is available online at stacks.iop.org/APEX/12/065003/mmedia). We further calculated the strain-caused energy shift of the QW by using deformation potential theory, and the calculated results agree well with the experimental results, as shown in the inset of Fig. 2(a). The results illustrate that the two QWs locate on opposite sides of the boundary line and are under different strain statuses, which will produce the sub-peaks with certain shift associating with rolled-up curvature changes. Our calculation illustrates that the inclination angle of conduction band edge increases with the decreasing diameter of the self-rolled-up nanomembrane. Therefore, the strain status and corresponding shift of energy levels can be easily tuned by altering the diameter of the tubular structure, and thus the

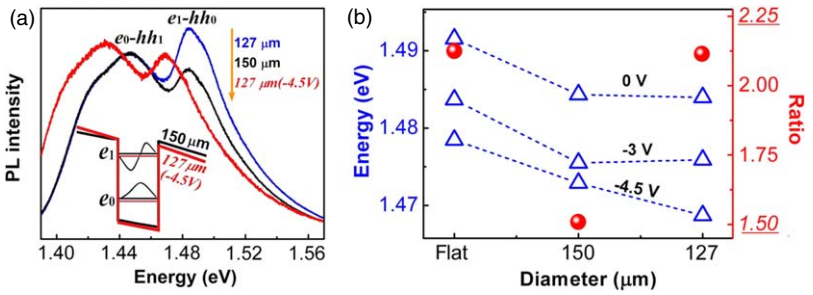

Fig. 3. (Color online) (a) PL spectra of self-rolled-up nanomembranes with diameters of 127 and 150 μm at room temperature. Bias voltage of −4.5 V was also applied to 127 μm tube. The inset shows the band structures of 150 and 127 μm (−4.5 V applied) tubes. (b) Open triangle (left vertical axis) indicates the energy values of e_1-hh_0 transitions for flat and self-rolled-up nanomembranes with diameters of 150 and 127 μm. Bias voltages of 0, −3, and −4.5 V were applied to the nanomembranes. Solid circles (right vertical axis) indicate the ratio of emission energy shift under −4.5 V bias to that under −3 V bias for e_1-hh_0 transition.

spectral responses of devices can be modulated by producing rolled nanomembranes with different geometrical parameters.

Obviously, the change of band structure in such self-rolled multi-layered nanomembranes is quite complicated, and in order to go deeper into this, the band structures of the devices were studied by means of PL characterization. Here, the ground and the first excited states of electron are marked as e_0 and e_1 while hh_0 and hh_1 for heavy hole (hh) case. The recombination between the electrons (e) and the hh brings about the two obvious PL peaks (e_0-hh_1, e_1-hh_0) in Fig. 3(a) and the shift of the peaks is ascribed to the changes of ground state(e_0) and excited state(e_1).[1,20,22] One may note that the energy shifts of QW1 and QW2 should depend on the strain direction,[23–25] and the optical transitions in QW1 and QW2 are different. However, this difference should be significantly smaller compared with the linewidth of the PL peak [see supplementary material A and Fig. 3(a)], making the difference indistinguishable in present PL characterization. Thus, the peaks in Fig. 3(a) are actually from transitions in both QW1 and QW2. In addition, we also applied bias voltage to the self-rolled-up nanomembrane (diameter: 127 μm) when the PL signal was collected. It can be seen from Fig. 3(a) that both e_0-hh_1 and e_1-hh_0 peaks redshift after voltage is applied and the shift is mainly caused by the downward moving of the band levels in biased QWs.[12] Furthermore, as shown in the inset of Fig. 3(a), the applied electric field can also cause the deviations of the wave functions for the ground state (moving to right) and the excited state (moving to left), which modifies the superimposed wave function to change the relative intensities of the peaks.[26] Accordingly, it can be found in Fig. 3(a) that the e_0-hh_1 peak is larger than e_1-hh_0 peak for the 127 μm sample with -4.5 V applied voltage, which is different from 127 μm sample without applied voltage.

Different bias voltages (i.e., -4.5 and -3 V) were applied to flat and self-rolled nanomembranes to study the shift of e_1-hh_0 peak [Fig. 3(b)]. The ratios of the shifts under -4.5 V to that under -3 V were calculated to be more close to the square of the voltage ratio (i.e., 2.25) for the flat nanomembrane and self-rolled-up nanomembrane with diameter of 127 μm, while for self-rolled-up nanomembrane with diameter of 150 μm, the ratio is close to the voltage ratio (i.e., 1.5). It can be deducted that the first order Stark effect due to obvious electric dipole moment exists in 150 μm sample. The flat nanomembrane and 127 μm samples are inclined to the second order Stark effect.[27] These results can also be drawn from the shift of e_0-hh_1 peak by the same calculation method (see supplementary material B). Here, the Stark effect is induced by the stress in the GaAs and $Al_{0.26}Ga_{0.74}As$ layers,[28] and the internal electric field in 150 μm sample can shift the wave function just as in the case of 127 μm sample with applied voltage of -4.5 V to produce the similar line shape (e_0-hh_1 peak is a little higher).

The total potential of electrons could be coupled by deformation potential and piezoelectric potential.[29] For rolled nanomembrane, the radius (R_0) with bending momentum (M_0) and certain thickness (t) can be expressed as follows

$$R_0 = D/M_0 = t/((1+\nu)\Delta\varepsilon), \quad (1)$$

where D is the stiffness of the nanomembrane, ν represents Poisson ratio, $\Delta\varepsilon$ is the strain gradient.[30] The formula manifests that the tubular structure with different diameter can lead to different strain gradients and deformation potentials to affect the depth of the minima of total potential energy for electrons. For 150 μm rolled-up nanomembrane, the first order Stark effect means the electrons in QWs have high polarization energy (i.e. electrostatic potential energy), which means the potential minima does not locate at QWs to exhibit obvious polarization effect. Comparably, for 127 μm sample, the second order Stark effect means the potential minima locates at QWs because of the faintest polarization energy without observable polarization effect.

The Stark effect will affect the properties of photodetectors based on QWs.[28] The polarization induced by strain will affect the transport properties of carriers to change the carrier concentration and mobility, and then the photoelectric responsivity of the device will be affected.[31,32] To study the influence of polarization, we further studied the properties of self-rolled nanomembrane with different geometries. As can be seen from Fig. 4, the blackbody responsivity of the smaller tube (diameter: 62 μm) is 2.3 times larger than that of flat nanomembrane, which is mainly due to the increased reflections in the tubular structure and the absorption of the incident light is significantly enhanced.[11] The corresponding performance of the device is also influenced. Moreover, it is worth noting that the rolling process minimizes the strain energy of the nanomembrane. Previous literature 16) concerning $In_{0.2}Al_{0.2}Ga_{0.6}As$ strain layer indicated that the discrepancy of ultimate strain energies in rolled-up and rolled-down nanomembranes are very small. Interestingly, in our experiment, we experimentally found that when the HF concentration is higher than 10%, the nanomembrane intends to roll up, otherwise the nanomembrane prefer downward rolling. This is because that a low etching rate further increases possibility of producing self-rolled-down tubes.[20] Here, we removed the AlAs sacrificial layer in 8% HF for 5 min to get a self-rolled-down nanomembrane(D-tube for short) for further investigation. Under the same test conditions, the blackbody responsivity of D-tube is almost 3.5 times higher than that of the flat nanomembrane, which is also ~52% enhancement compared with the self-rolled-up nanomembrane (Fig. 4). The reasons can be listed as follows. Firstly, applied stress leads to the energy level splitting of the conduction band.[33] Tensile strain increases the binding

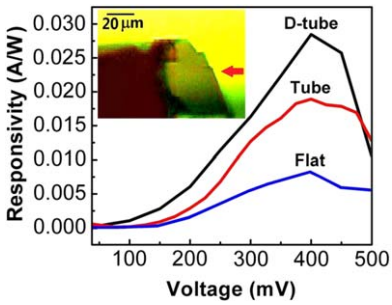

Fig. 4. (Color online) Comparison of blackbody responses for self-rolled nanomembranes and the 45° edge-facet flat nanomembrane. D-tube represents a self-rolled-down nanomembrane with the diameter of ~78 μm. Tube represents a self-rolled-up nanomembrane (diameter: 62 μm). The inset is the optical image of the D-tube device. The red arrow points to the self-rolled-down nanomembrane.

energy of the lowest sub-band, which enlarges the number of photoelectrons on the conduction band, and the lifetime of the photoelectrons increases correspondingly. On the contrary, compressive stress decreases the binding energy of the lowest sub-band, which reduces the number of photoelectrons on the conduction band.[33,34)] Secondly, applied stress affects the generation and recombination rates of electrons and holes,[35)] and the effects of strain on carrier concentration and transport characteristics are different.[36)] The tensile strain leads to larger lattice spacing and lower scattering possibility of carriers, which causes low device noise and high responsivity. Comparably, the compressive strain leads to high noise and low responsivity because of the smaller lattice spacing and higher scattering possibility.[34)]

In conclusion, we have studied the band structure and opto-electrical properties of self-rolled QW-contained nanomembranes with different diameters by means of photoelectric response characterization and PL measurement. Both experimental and theoretical investigations demonstrate the possibility of modulating the photocurrent response of the devices by tuning the diameters of the self-rolled structures and the band structures are regulated correspondingly. The PL spectra at room temperature further elucidate the interfacial polarization in self-rolled nanomembranes. Detailed spectral analyses suggest that the responsivity of tensed QW is higher than QW in compressive strain. Thus, the self-rolled-down nanomembrane exhibited even higher blackbody responsivity: the responsivity is almost 3.5 times higher than that of the 45° edge-facet flat nanomembrane and is ∼52% higher than that of the self-rolled-up nanomembrane. These conclusions will facilitate the development of infrared detectors with good thermal stability, wide viewing angle, high sensitivity, and broad-spectrum absorption.

Acknowledgments This work was financially supported by the National Natural Science Foundation of China (Nos. 61728501 and 61805042), the China Postdoctoral Science Foundation (No. 2018M632014), the Science and Technology Commission of Shanghai Municipality (Nos.18ZR1405100 and 17JC1401700), the Program of Shanghai Academic/Technology Research Leader (16XD1404200), and the Changjiang Young Scholars Program of China.

ORCID iDs GaoShan Huang https://orcid.org/0000-0002-0525-7177 YongFeng Mei https://orcid.org/0000-0002-3314-6108

1) I. S. Makhov, V. Y. Panevin, A. N. Sofronov, D. A. Firsov, L. E. Vorobjev, M. Y. Vinnichenko, A. P. Vasil'ev, and N. A. Maleev, Superlattices Microstruct. **112**, 79 (2017).
2) Z. Cevher, P. A. Folkes, H. S. Hier, B. L. VanMil, B. C. Connelly, W. A. Beck, and Y. H. Ren, J. Appl. Phys. **123**, 161512 (2018).
3) Q. Li, Z. F. Li, N. Li, X. S. Chen, P. P. Chen, X. C. Shen, and W. Lu, Sci. Rep. **4**, 6332 (2014).
4) F. Li and Z. Mi, Opt. Express **17**, 19933 (2009).
5) D. Brick et al., Sci. Rep. **7**, 5385 (2017).
6) A. Muller, W. Fang, J. Lawall, and G. S. Solomon, Phys. Rev.Lett. **103**, 217402 (2009).
7) X. L. Li, Adv. Opt. Photonics **3**, 366 (2011).
8) H. P. Ning, Y. Zhang, H. Zhu, A. Ingham, G. S. Huang, Y. F. Mei, and A. Solovev, Micromachines **9**, 75 (2018).
9) W. Huang, X. Yu, P. Froeter, R. Xu, P. Ferreira, and X. Li, Nano Lett. **12**, 6283 (2012).
10) V. Y. Prinz, E. V. Naumova, S. V. Golod, V. A. Seleznev, A. A. Bocharov, and V. V. Kubarev, Sci. Rep. **7**, 43334 (2017).
11) H. Wang, H. L. Zhen, S. L. Li, Y. L. Jing, G. S. Huang, Y. F. Mei, and W. Lu, Sci. Adv. **2**, e1600027 (2016).
12) J. H. Wong, B. R. Wu, and M. F. Lin, J. Phys. Chem. C **116**, 8271 (2012).
13) Y. F. Mei, S. Kiravittaya, M. Benyoucef, D. J. Thurmer, T. Zander, C. Deneke, F. Cavallo, A. Rastelli, and O. G. Schmid, Nano Lett. **7**, 1676 (2007).
14) C. Strelow, C. M. Schultz, H. Rehberg, M. Sauer, H. Welsch, A. Stemmann, C. Heyn, D. Heitmann, and T. Kippl, Phys. Rev. B **85**, 155329 (2012).
15) V. Y. Prinz, V. A. Seleznev, A. K. Gutakovsky, V. V. Preobrazhenskii, M. A. Putyato, and T. A. Gavrilova, Phys. E **6**, 828 (2000).
16) S. Bhowmick, T. Frost, and P. Bhattacharya, Opt. Lett. **38**, 1685 (2013).
17) K. M. Schulz, H. Vu, S. Schwaiger, A. Rottler, T. Korn, D. Sonnenberg, T. Kipp, and S. Mendach, Phys. Rev. Lett. **117**, 085503 (2016).
18) A. Malachias, C. Deneke, B. Krause, C. Mocuta, S. Kiravittaya, T. H. Metzger, and O. G. Schmidt, Phys. Rev. B **79**, 03531 (2009).
19) R. M. Costescu, C. Deneke, D. J. Thurmer, and O. G. Schmidt, Nanoscale Res. Lett. **4**, 1463 (2009).
20) H. L. Zhen, G. S. Huang, S. Kiravittaya, S. L. Li, C. Deneke, D. J. Thurmer, Y. F. Mei, and O. G. Schmidt, Appl. Phys. Lett. **102**, 041109 (2013).
21) C. G. V. D. Walle, Phys. Rev. B **39**, 1871 (1989).
22) X. L. Zeng, J. L. Yu, S. Y. Cheng, Y. F. Lai, Y. H. Chen, and W. Huang, J. Appl. Phys. **121**, 193901 (2017).
23) T. B. Bahder, Phys. Rev. B **41**, 11992 (1990).
24) O. Stier, M. Grundmann, and D. Bimberg, Phys. Rev. B **59**, 5688 (1999).
25) P.-L. de Assis et al., Phys. Rev. Lett. **118**, 117401 (2017).
26) H. Q. Le, J. J. Zayhowski, and W. D. Goodhue, Appl. Phys. Lett. **50**, 1518 (1987).
27) H. Haken and H. C. Wolf, *The Physics of Atoms and Quanta* (Springer, Herdelberg, 2005).
28) A. Pateras et al., Nano Lett. **18**, 2780 (2018).
29) J. H. Davies, J. Appl. Phys. **84**, 1358 (1998).
30) C. Peter, K. Suwit, M. Ingolf, S. Joachim, and G. S. Oliver, Nano Lett. **11**, 236 (2011).
31) L. S. Vanasupa, M. D. Deal, and J. D. Plummer, Appl. Phys. Lett. **55**, 274 (1989).
32) A. K. Fung, J. D. Albrecht, M. I. Nathan, P. P. Ruden, and H. Shtrikman, J. Appl. Phys. **84**, 3741 (1998).
33) W. T. Masselink, Y. C. Chang, and H. Morkoc, Phys. Rev. B **32**, 5190 (1985).
34) J. S. Harris, J. L. Moll, and G. L. Pearson, Phys. Rev. B **1**, 1660 (1970).
35) W. Fulop and S. Konidaris, Solid State Electron. **19**, 313 (1976).
36) Y. Saito, J. Appl. Phys. **71**, 3544 (1992).